Molecular Dynamics Simulations of Ternary Membrane Mixture: Phosphatidylcholine, Phosphatidic Acid, and Cholesterol

Mary Hongying Cheng,[†] Lu Tian Liu,[‡] Alexander C. Saladino,[‡] Yan Xu,[‡,§] and Pei Tang*[,‡,§,||]

Departments of Anesthesiology, Pharmacology, and Computational Biology, University of Pittsburgh School of Medicine, and Department of Chemistry, University of Pittsburgh, Pittsburgh, Pennsylvania 15261

Received: July 12, 2007; In Final Form: September 4, 2007

A ternary mixture of 1-palmitoyl-2-oleoyl phosphatidylcholine (POPC), 1-palmitoyl-2-oleoyl phosphatidic acid (POPA), and cholesterol (CHOL) works effectively for a functional conformation of nicotinic acetylcholine receptor (nAChR) that can undergo agonist-induced conformation changes, but POPC alone can stabilize only a desensitized state of nAChR. To gain insights into the lipid mixture that has strong impact to nAChR functions, we performed more than 50 ns all atom molecular dynamic (MD) simulations at 303 K on a fully hydrated bilayer consisting of 240 POPC, 80 POPA, and 80 CHOL (3:1:1). The MD simulation revealed various interactions between different types of molecular pairs that ultimately regulated lipid organization. The heterogeneous interactions among three different constituents resulted in a broad spectrum of lipid properties, including extensive distributions of average area per lipid and varied lipid ordering as a function of lipid closeness to CHOL. Higher percentage of POPA than POPC had close association with CHOL, which coincided with relatively higher ordering of POPA molecules in their acyl chains near lipid head groups. Lower fraction of gauche dihedrals was also found in the same region of POPA. Although the CHOL molecules had the effects on the enhancement of surrounding lipid order, relatively low lipid order parameters and high fraction of gauche bonds were observed in the ternary mixture. Collectively, these results suggest that the dynamical structure of the ternary system could be determinant for a functional nAChR.

Introduction

The membrane lipid composition often has critical effects on structure stability and functions of membrane proteins.[1] The nicotinic acetylcholine receptor (nAChR) from Torpedo is one of such examples.[2] Each subunit of this pentameric neurotransmitter gated receptor has a large extracelluler domain with an agonist binding site and four transmembrane domains. The second transmembrane domain lines the pore of the channel. Other transmembrane domains, especially the fourth transmembrane domain, are expected to interact with lipids.[3,4] When the nAChR is in a functional resting state, the channel can be opened by agonists binding and allows ions translocation through the channel. However, if the receptor is reconstituted not with a proper lipid composition, such as in phosphatidylcholine (PC) alone, the channel will not be able to activate and appears to be in a desensitized state.[5] The anionic lipid phosphatidic acid (PA) and cholesterol (CHOL) are proved to be critical components to restore nAChR's full functionality, including ligand binding and ion translocation, in reconstituted lipid mixtures.[6−10] Other anionic lipids, such as phosphatidylserine (PS) and phosphatidylinositol (PI), showed lower efficacy than PA in stabilizing nAChR in the resting state, though they are much more abundant in native membranes.[10,11]

Despite extensive experimental validations of the necessity of PA and CHOL for functional nAChRs, it is still obscure, at molecular level, how PA and CHOL affect membrane properties that ultimately modulate the functionality of nAChR. The functional requirement of the nAChR for PA and CHOL was proposed to stem from the binding of specific lipids to distinct sites on the nAChR either to affect nAChR secondary structure[12,13] or to modulate the equilibrium between the resting and the desensitized states of nAChR.[14] It was suggested in these studies that the rigid sterol ring of CHOL could intercalate into the grooves of nAChR α helices to stabilize transmembrane structures of the nAChR, whereas the negatively charged headgroup of PA might have electrostatic interactions with positive charged residues of the nAChR. Direct interaction of these molecules with the nAChR was proposed to account for the requisite specific lipid composition for receptor functions. However, several lines of experimental evidence have later emerged to an alternate mechanism that CHOL, PA, or both may act on the nAChR via an indirect effect on some physical properties of the lipid bilayer.[5,10,15] Both CHOL and PA are able to increase the lateral packing density of the lipid bilayers, which could lead to slow nAChR internal motion.[5,16] Although collective influence of CHOL and PA on the physical properties of lipid mixtures can be experimentally characterized, experimental elucidation of molecular details on how CHOL and PA impose their effects remains challenging.

Molecular dynamics (MD) simulation has emerged as a useful tool to complement experimental efforts for a comprehensive understanding of structures and dynamics of various lipid systems.[17−19] Along with recent advancement in computational power, atomistic simulations of lipid or mixed lipid systems with long time and length scales become realistic. In this study, we generated a ternary lipid system comprising of 1-palmitoyl-2-oleoyl phosphatidylcholine (POPC), 1-palmitoyl-2-oleoyl

* Corresponding author. E-mail: tangp@anes.upmc.edu. Address: 2049 Biomedical Science Tower 3, 3501 Fifth Avenue, University of Pittsburgh, Pittsburgh, Pennsylvania 15261. Phone: (412) 383-9798. Fax: (412) 648-8998.

[†] Department of Chemistry.

[‡] Department of Anesthesiology.

[§] Department of Pharmacology.

[||] Department of Computational Biology.

10.1021/jp075467b CCC: $37.00
Published on Web 12/05/2007

phosphatidic acid (POPA), and CHOL in a 3:1:1 molar ratio. The composition of the ternary system mimics the lipid requirement for a functional nAChR.[9] The size of the bilayer is large enough to embed a whole nAChR for further studies. A more than 50 ns all-atom MD simulation was preformed in the present study to gain insight into this ternary mixture that might be relevant to the modulation of nAChR functions.

Methods

System Preparation. A large hydrated ternary lipid patch ($120 \times 120 \times 55$ Å) was generated by replicating and truncating a smaller ternary system ($46.5 \times 46.5 \times 55$ Å) that was modified from a same size POPC patch (30 POPC per leaflet) provided in the membrane package by the VMD program.[20] Among 30 POPC lipids in each original monolayer, 6 were modified into POPA lipids, and another 6 were replaced by CHOL molecules. Because of their structure similarity, the POPA structure was created by replacing the choline headgroup of POPC with a hydrogen atom. The structure of CHOL molecules was taken from the crystal structure of the hRORα LBD-CHOL complex (pdb code: 1N83).[21] This small ternary lipid patch was replicated nine times to generate a large batch. Since we wanted to keep the lipid patch large enough for embedding a whole nAChR but small enough without wasting computational power for excess number of lipids in the system, we trimmed off some lipid molecules along two edges of the lipid patch. The locations of POPA and CHOL were determined by maximizing their random distribution in POPC and making a more homogeneous mixture. The vertical positions of cholesterols parallel to membrane normal were adjusted to maximize the chance of hydrogen bonding between their hydroxyl oxygen atoms and the carbonyl oxygens of the POPC and POPA molecules.

The prepared large ternary lipid patch has the 3:1:1 molar ratio of POPC, POPA, and CHOL to mimic the composition requirement of the lipid mixture for functional nAChRs.[9] Sodium and chloride ions were added into the system by replacing water molecules to produce ionic concentrations of 150 mM. Additional sodium ions were introduced to the system to counter-balance the negative charges of the POPA lipids. The final system has 80 898 atoms, including 240 POPC, 80 POPA, 80 CHOL molecules, 11 132 waters (27.8 waters per lipid), 111 Na^+, and 31 Cl^- ions.

The CHARMM27[22] force field provides the parameters for POPC. The parameters of POPC were adopted for POPA except that the charges of oxygen atoms in the phosphate group were adjusted slightly to make a -1 charge for POPA. The recently reported parameters of cholesterol[23] were applied in the present study. A 10 000 step energy minimization was performed on the system using a conjugate gradient and line search algorithm to remove energetically unfavorable contact points. The system was equilibrated under the condition of constant volume and temperature (303 K) and further under the condition of constant pressure (one bar) and temperature (303 K). The program of NAMD 2.5 (http://www.ks.uiuc.edu/Research/namd)[24] was used for the system energy minimization and atomistic MD simulations.

Molecular Dynamics Simulations. The Nosé−Hoover Langevin piston pressure control[25,26] and the Langevin damping dynamics[27] were used to keep the system under 1 atm constant pressure and 303 K constant temperature, respectively. Water wrapping, SHAKE routine with a tolerance of 10^{-6} Å, and periodic boundary conditions were utilized during simulations. The time step was 1 fs for the initial 1 ns simulation and was extended to 2 fs afterward. The bonded interactions and the short−range nonbonded interactions between particles within 10 Å were calculated at every time step. The long−range electrostatic forces were calculated every four time steps with the particle mesh Ewald (PME).[28] The pair list of the nonbonded interaction was updated every 20 time steps with a pair list distance of 11.5 Å. The energies and trajectories were stored every 500 and 2000 time steps for subsequent data analysis. Over 50 ns NPT MD simulations were performed on the system.

Data Analysis. Majority part of data analysis used the scripts developed within the VMD software environment[20] on a local Linux computer. Lipid order parameter was characterized from the simulation trajectory using the following equations I and II:[29,30]

$$S_n = \langle (3\cos^2\beta_n - 1)/2 \rangle \quad \text{(I)}$$

$$|S_n^{CD}| = 0.5 S_n \quad \text{(II)}$$

where n denotes the nth carbon counted from the carbonyl carbon atom along the acryl chain, β_n is the angle between the membrane normal and the vector connecting an aliphatic carbon C_{n-1} with C_{n+1}. Brackets denote averaging over time and all the same type of molecules.

The radial distribution function (RDF) for various atom pairs in different lipids was used to identify pattern formations in our ternary lipids. The RDF, $g_{AB}(r)$ (simplified as $g(r)$), describes the probability of finding a particle B in a given distance from particle A:

$$g_{AB}(r) = \frac{1}{\langle \rho_B \rangle} \frac{1}{N_A} \sum_{i \in A}^{N_A} \sum_{j \in B}^{N_B} \frac{\delta(r_{ij} - r)}{4\pi r^2} \quad \text{(III)}$$

where N_A is the total number of particle A around particle B in the distance of r and $\langle \rho_B \rangle$ is the number density of particle B.

The area per lipid molecule for each molecule type was calculated using a home-developed code on the basis of the Voronoi tessellation method (http://www.cs.cmu.edu/~quake/triangle.html).[31] The detailed calculation procedure was similar to that reported previously for lipid mixtures.[32−35] To prevent the calculation from overestimating the area for smaller size CHOL or underestimating the area for larger molecules POPC and POPA, we also adopted the previously published method to generate Voronoi tessellation.[33] In brief, three atoms located at the hydrophobic/hydrophilic interface of each POPA (C2, C21, C31) or POPC (C1, C21, C32), as shown in Figure 1, were chosen to represent a lipid in a Voronoi tessellation. The CHOL, however, was represented by only hydroxyl oxygen (O3). The selected atoms were projected onto the $X-Y$ plane for constructing a Delaunay triangulation. The circumcenters were calculated for each of these triangles and offered the coordinates of the vertices of the Voronoi polygons. For an individual polygon, its vertices (or edges) were sorted according to their geometric sequence along the circumference of the polygon. A molecular polygon was formed by combining corresponding atomic polygons. Area per lipid was calculated as summation of all atomic polygons belonging to the same molecule.

Results and Discussions

Interactions among Three Constituents. Lateral interactions among constituents define packing properties of lipids that could impact directly on membrane protein functions. Figure 2 shows

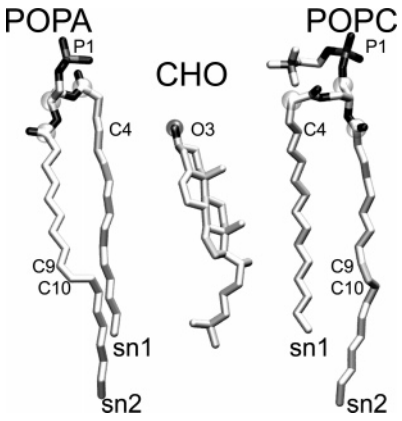

Figure 1. Structures of POPC, POPA, and CHOL molecules. Atoms selected for Voronoi tessellation are highlighted in spheres. Several atoms mentioned in the text and carbon atoms in the double bond are labeled.

top views of the system snapshots at the beginning and end of the 50 ns simulation. Several features became apparent at the end of the simulation. First, CHOL molecules were well-solvated by POPC or POPA. Second, some CHOL dimers were formed during the simulation, though individual CHOL molecules were separated at the beginning of the simulation. Third, intimate interaction between POPA and CHOL was increased dramatically over the course of simulation. Fourth, unlike POPC and CHOL, POPA molecules had no strong tendency to interact with each other. These visual observations were further confirmed and quantified using RDFs of phosphors (P1) of lipids and the hydroxyl oxygen (O3) of CHOL. As shown in Figure 3A,B, close interactions between POPA and CHOL were not obvious at the beginning of the simulation, but was well-established at ~30 ns and remained until the 50 ns simulation. The interactions were most populated at $\sim 3.7 \pm 0.5$ Å between P1 of POPA and O3 of CHOL molecules. POPC also showed its most popular interaction with CHOL at $\sim 3.7 \pm 0.5$ Å. The difference is that the probability of an intimate interaction with CHOL for POPC is not as high as for POPA. This is consistent with the hydrogen bonding analysis shown later in this article. Figure 3C demonstrates a stable association between POPC and POPA, as evidenced by the high distribution at the distance of $\sim 6.5 \pm 0.5$ Å between pairing phosphors of POPC and POPA through the simulation.

RDFs for the same type of molecules were summarized in Figure 3D,E for assessing domain formations of a particular molecular type. CHOL had two well-defined peaks at 5.5 and 10.5 Å after 30 ns simulations in Figure 3D. These peaks became less intensive in the following simulation, presumably because of competitive interaction of CHOL molecules with their adjacent phospholipids in the later stage of the simulation. RDFs of POPC (Figure 3E) at different simulation times were similar and the highest population of POPC−POPC was at ~6.5 Å. In contrast, a high population of close interactions between POPA molecules did not develop even at the end of simulation (Figure 3F), probably resulting from the repulsive Columbic interaction among the charged head group in POPA.

Figure 4 illustrated several examples of complexation pairs that were driven by different interactions. For POPA/CHOL or POPC/CHOL, strong van der Waals (VDW) interaction of CHOL seemed more favorable to the saturated lipid chain (sn1), as evidenced by more CHOL molecules in a close vicinity to sn1 chains than to unsaturated sn2 chains. The CHOL molecules also showed a preferred orientation with their methyl group facing away from their closely interacted lipids, as depicted in Figure 4A. The preference of the flat face of CHOL to a saturated lipid chain was also observed previously in the DOPC/SM/CHOL system and believed to be entropically favored for better packing of saturated lipid chains around CHOL molecules.[36,37] Besides the VDW interaction, the hydroxyl group of CHOL also formed hydrogen bonding with oxygen atoms (O1−O4) of the phosphate group or oxygen atoms (O31, O32, O21, O22) in the acryl chains of the lipids (Figure 4B). Among CHOL formed hydrogen bonds at 50 ns simulation, 24% and 12% were found with POPC and POPA, respectively. Given the fact that POPA was only one-third of the POPC quantity in the system, it seemed that CHOL was almost 1.5 times favorable to hydrogen bonding with POPA than POPC. The head group of POPA is shorter and much less bulky than that of POPC, probably making POPA less sterically hindered from interacting with CHOL. The rest of the hydrogen bonding of CHOL was largely with water molecules, producing a layer of less-mobile water in the lipid headgroup. A very small population of CHOL, as indicated by a little peak around 3 Å in Figure 3D, were hydrogen-bonded directly between hydroxyl groups of two CHOL molecules (Figure 4C). Hydrogen bonding was also found to be mediated via a water molecule (Figure 4D). The lifetime of CHOL dimers could last several hundred picoseconds in the simulation. As demonstrated in Figure 3C,E,F, most of lipids kept away from each other with a most popular distance of ~6 Å between P1 atoms. However, several pairs of POPA and POPC, as shown in Figure 4E, interact via Columbic interaction between negative charged phosphate group of POPA and positive charged nitrogen atom (N) of choline moiety of POPC. The lipid pairs formed through Columbic interaction were also observed in other lipid simulation systems previously.[38,39] Figure 4F shows an example of Na^+ mediated POPA−POPC complex that lasted for several nanoseconds in the simulation.

The formation of various complexes through diverse interactions could be the basis for a dynamic structure of the lipid bilayer that is further analyzed in the following sections.

Average Area per Molecule. The average area per lipid molecule is one of the parameters that quantify the lateral structure of a lipid system. For our simulated POPC−POPA−CHOL system, the area per molecule for each constituent in the ternary mixture was calculated using the aforementioned Voronoi method[31] and summarized in the histograms depicted in Figure 5. Several features of these histograms are worth noting. First, the area per molecule is rather heterogeneous than uniform among three constituents. The area per POPA or POPC distributes broader than the area per CHOL, which is consistent to the fact that both POPC and POPA have more flexible structures than CHOL. The inhomogeneous interaction among different constituents, as aforementioned, may be responsible for a heterogeneous area per molecule in the mixed bilayer. Second, the lateral system compression occurred at the early stage of simulations. The total $x-y$ area for each leaflet of the bilayer changed from its starting 120×120 Å^2 to 110×110 Å^2 after 20 ns simulations and then became stable for the rest of simulations. Such lateral compression was also reflected in Figure 5, where the highest population in the histograms of POPC, POPA, and CHOL after 50 ns simulations moved to the lower values of area per molecule in comparison to the corresponding data acquired at 10 ns simulations. Third, it is unrealistic to compare all of the results in Figure 5 with experimental data because of their unavailability, but the most populated area per POPC in the histogram for the system of 50 ns simulations seems smaller than the experimental value of

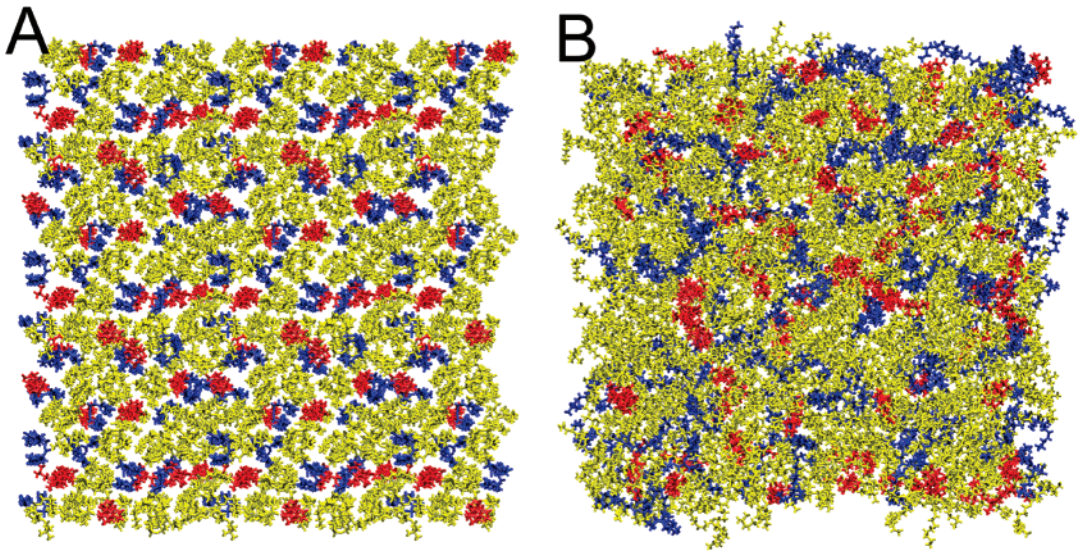

Figure 2. Top views of snapshots of the system experienced (A) 0 ns and (B) 50 ns MD simulations. Water molecules were removed for clarity. CHOL, POPA, and POPC are in red, blue, and yellow, respectively.

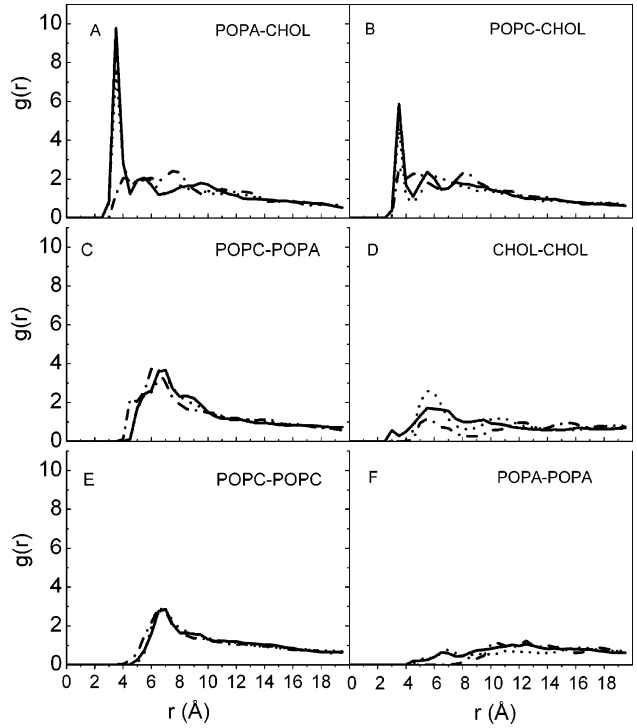

Figure 3. Radial distribution functions (RDF) between specified atom pairs after 1 ns (dash doted), 30 ns (short dashed), and 50 ns (solid line) simulations. (A) P1 atom of POPA vs O3 atom of CHOL; (B) P1 atom of POPC vs O3 atom of CHOL; (C) P1 atom of POPC vs P1 atom of POPA; (D) O3−O3 in CHOL; (E) P1−P1 in POPC; (F) P1−P1 in POPA. The data resulted from the average over 500 simulation frames near the designated simulation time.

68.3 ± 1.5 Å^2 obtained for a pure POPC preparation.[40] Smaller area per POPC molecule was also found in previous MD simulations for pure POPC and POPC mixture with CHOL.[33,41] The most populated area per POPA is similar to that for POPC, presumably because of the structure similarity in their hydrocarbon chains. The area per CHOL for the system equilibrated for 50 ns is 30 Å^2, which is close to the previously reported values of area per CHOL in the DOPC/SM/CHOL ternary mixture using the same Voronoi method.[33,36]

The choice of calculation methods may affect values of area per molecule. The resulting discrepancy can be significant, as reported in a recent study of POPC.[41] For ternary mixtures, the Voronoi method is often adopted for practical reasons rather than the accuracy of the method itself. One of major concerns with regard to the method is that the entire area is assigned to molecules in the Voronoi tessellation. The assumption of no free area in lipid is obviously unphysical and may artificially increase values of area per molecule. The recently developed partial-specific-area formalism[42] could avoid certain arbitrary factors, such as number of atoms chosen for tessellation, to offer more accurate results. The condensing effect of CHOL on lipid bilayers has been well-demonstrated using this method.[41,42] However, the partial-specific-area approach requires multiple MD simulations with several varied mole fractions of lipid compositions. Therefore, one cannot take this approach if MD simulations have been performed under only one condition of lipid constituents, such as the case in the current study.

The broadness of distribution of average area per molecule for each type of molecule in Figure 5 might imply that a single value was not adequate to capture essential structural and dynamical features of a complex system. The data analysis on order parameters of POPA and POPC in the following section supported the notion.

Lipid Ordering. The lipid ordering in the ternary system was measured using both order parameters and the fraction of gauche dihedral angles (defined here as between 50° and 70° or between −50° and −70°) along the hydrocarbon chains. The POPA and POPC showed similar flexibility in their sn1 chain tail region as measured by the order parameter S^{CD} in Figure 6A, but the POPA seemed to be more rigid than POPC in the head region. To prove that higher absolute magnitude of S^{CD} for POPA resulted from more intimate interaction of POPA with CHOL, we counted the number of POPA molecules whose C4 atoms (C4 showed the highest order parameter in our system) had a distance less than 3.5 Å from CHOL molecules and calculated their S^{CD}. We found that ∼20% POPA belonged to this category. The elevated S^{CD} for the selected POPA showed strong dependence on the distance to CHOL (cf. Figure 1S in Supporting Information), confirming that well recognized CHOL effect on lipid ordering[37,43] also existed in the current simulation. We found only ∼15% POPC molecules in close contact to CHOL if using the same criterion. Therefore, higher S^{CD} values for overall POPA molecules reflected their higher probability

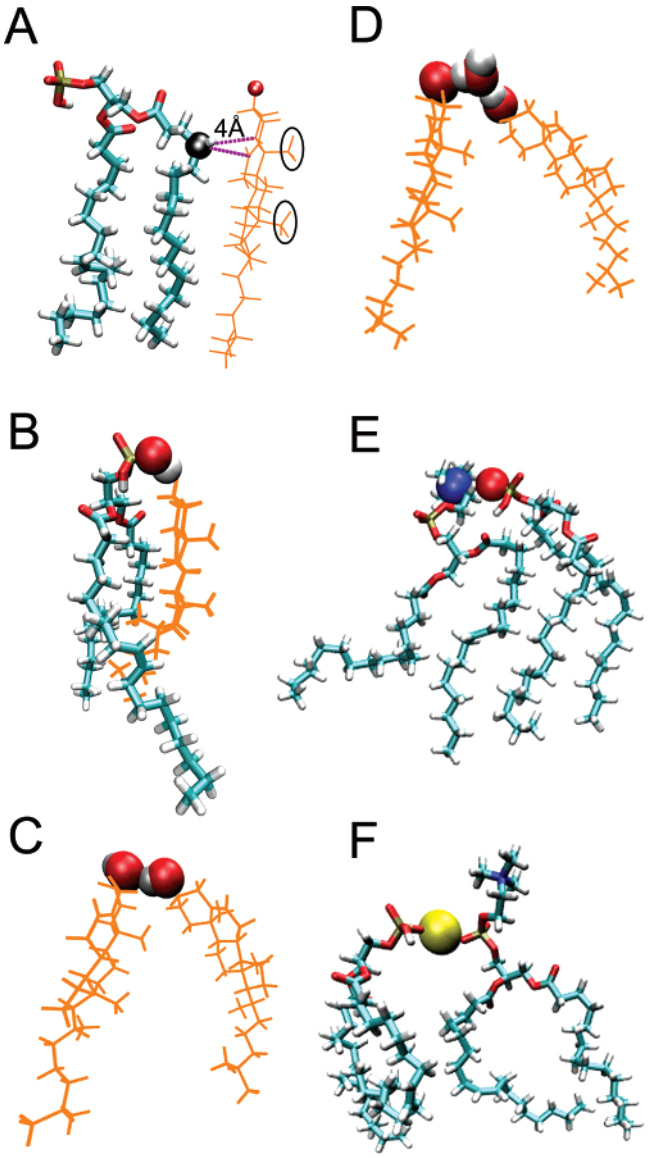

Figure 4. Snapshots of various interacting pairs in the POPC−POPA−CHOL system: (A) VDW interaction of POPA and CHOL (orange). Two methyl groups on the rings of CHOL are highlighted in circle. Black sphere in POPA represents C4 atom in sn1 chain. (B) hydrogen bonding (HB) between POPA and CHOL; (C) HB between two CHOL molecules; (D) water mediated HB between CHOL molecules; (E) electrostatic interaction between headgroup oxygen of POPA (red) and nitrogen of choline group of POPC (blue); (F) Na^+ (yellow) mediated pairing between POPA and POPC.

than POPC to interact with CHOL, which agreed well with the observation in Figure 3A,B.

Figure 6B shows several POPC ordering profiles at different simulation times. The ordering pattern became stable after 30 ns simulation, as indicated by highly resembled data from the 30 and 50 ns simulations. It was noticeable that C4 did not have markedly higher S_4^{CD} value than its neighboring carbons until at a later stage of the simulation. The same phenomenon was also observed in POPA. The timeline for developing substantially high S_4^{CD} matched well with the growth of POPA or POPC paring with CHOL shown in Figure 3A,B, suggesting that the strong interaction of C4 with CHOL might be responsible for the notably higher S_4^{CD}. A close inspection revealed that C4, in most cases, was located below the level of hydroxyl of CHOL and aligned with the ring of CHOL, which may facilitate the C4 rigidness.

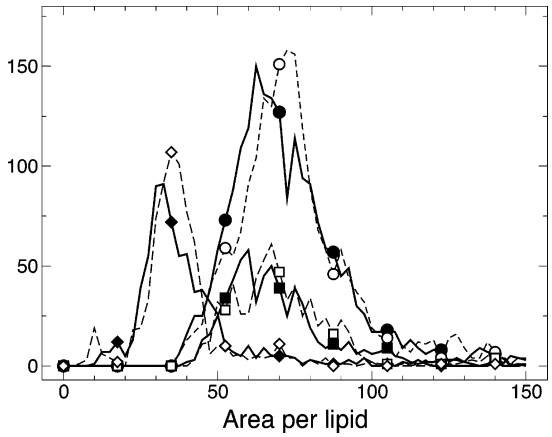

Figure 5. Histograms of area per molecule for the system experienced 10 ns (dash lines with open symbols) and 50 ns (solid lines with solid symbols) MD simulations. Each histogram, with a bin size of 2.5 Å^2, resulted from averaging both leaflets in 10 representative simulation snapshots over 40 ps time slabs. Individual components included POPC (●), POPA (■), CHOL (♦). For clarity, most of the symbols were not shown in the plots.

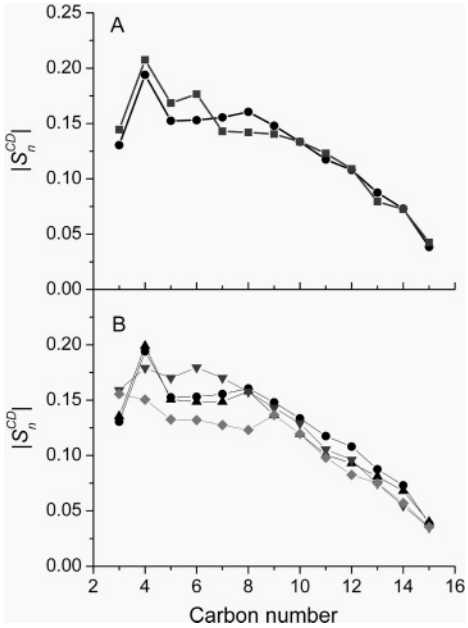

Figure 6. Comparison of order parameters for (A) the sn1 chains of POPC (●) and POPA (■) at 50 ns and (B) POPC at a number of simulation time point: 10 ns (♦), 15 ns (▼), 30 ns (▲), and 50 ns (●). The reported S_n^{CD} resulted from the average over 500 simulation frames near the designated simulation time. The error bars are smaller than the symbol size.

Although CHOL had positive impact on the lipid ordering, the overall absolute magnitude of order parameters in the current system were compatible to the previous POPC simulation without CHOL[44] or lower than that for a POPC−CHOL system with a similar percentage of CHOL.[41] Gauche defects were suspected to be responsible for lipid disordering. A low gauche fraction is indicative of a high ordering or vice versa. Therefore, we assessed the gauche defects by measuring the fraction of gauche dihedrals in the lipid chains. The detailed result is provided in Figure 2S in Supporting Information and is consistent with previous studies on mono-unsaturated lipids in the absence of CHOL.[45,46] The averaged number of gauche bonds in each chain was 4.2 for the lipid sn1 chains and 3.9 and 4.0 for sn2 of POPA and POPC, respectively. In comparison to those found for saturated lipids systems,[47−49] the ternary

mixture had on average one more gauche bond per lipid chain, suggesting that the gauche defects could be leading cause for the high mobility of the lipid acyl chains in our system.

The dependence of lipid ordering on lipid packing has been studied extensively in the past. It was elegantly demonstrated from POPC MD simulations that S_4^{CD}could fall from 0.2 to 0.13 when the area per POPC was manipulated to expand from 64 to 74 (Å^2).[44] Thus, a more tightly packed initial lipid system would likely result in higher ordered lipids. The length of simulation time could also affect dynamic structures of lipids. Although 50 ns for the current simulation is longer than times used for the majority of published MD simulations, one can always wonder if a much longer simulation time is necessary to accurately capture the true dynamic structure of the ternary system. Since our data obtained at a 50 ns simulation showed high similarity to the data at 30 ns, a longer simulation time within our reachable computational power seems unlikely to produce significant difference from our current outcome.

The correlation between bulk lipid ordering and nAChR function is not obvious based on previous experimental studies.[9,50] The nAChR in 3:2 POPC/POPA appears to be predominately in a resting like state that is capable of undergoing agonist-induced desensitization. In contrary, the nAChR in 3:2 POPC/CHOL seems to be predominately desensitized (nonfunctional), even though the 3:2 POPC/CHOL membrane exhibits higher ordering than 3:2 POPC/POPA. Hence, the lipid ordering is unlikely a dominant factor that affects the protein functions. The requirement of the presence of both PA and CHOL for fully functional nAChR[9,11] implies the importance of potential interplay between PA and CHOL. Although it is impossible to assess synergetic effects of POPA and CHOL on nAChR in a system without the presence of nAChR, the close interactions of POPA and CHOL observed in our current system implicated the possibility for producing their synergetic effects and the necessity for further investigation along the line.

Electron Densities. Figure 7 shows the electron density profiles of water and lipids across the bilayer. The water density at $z = \pm 30$ Å represented the density of bulk water ($\sim 0.99 \pm 0.01$ g/cm^3 in Figure 3S. See Supporting Information). The water density was depleted to near zero at $z = \pm 10$ Å, showing water penetration into the currently simulated bilayer at a similar depth as that observed in the previously simulated pure POPC system.[51] The electron density profile of POPC in the current system resembles the profile of pure POPC,[51] showing maximum electron densities of lipid head groups at $z = \pm 15$ Å. Therefore, the thickness of POPC in our ternary mixture and in the pure POPC system[51] is essentially the same, which makes the mechanism[52] that CHOL regulates protein−lipid hydrophobic matching by increasing the lipid bilayer thickness unlikely applicable to nAChR in the ternary mixture. The maximum electron density for POPA occurs at almost same location along the bilayer normal as that for POPC, indicating good alignment of the phospholipid headgroups of POPC and POPA. The locations of several atoms of lipids and CHOL along the bilayer normal are demonstrated in Figure 7B. The phosphorus atoms (P1) in the two leaflets are about 38 Å apart and well water-hydrated in both POPC and POPA. The oxygen atoms (O3) in the hydroxyl of CHOL are significantly deeper into the bilayer and have more limited exposure to water. The C4 atoms of POPA and POPC, which had marked higher order parameter than other neighboring carbons (Figure 6), are about ~4 Å more toward bilayer center than where the CHOL hydroxyl (O3) is located, confirming that the ring structure of CHOL molecules

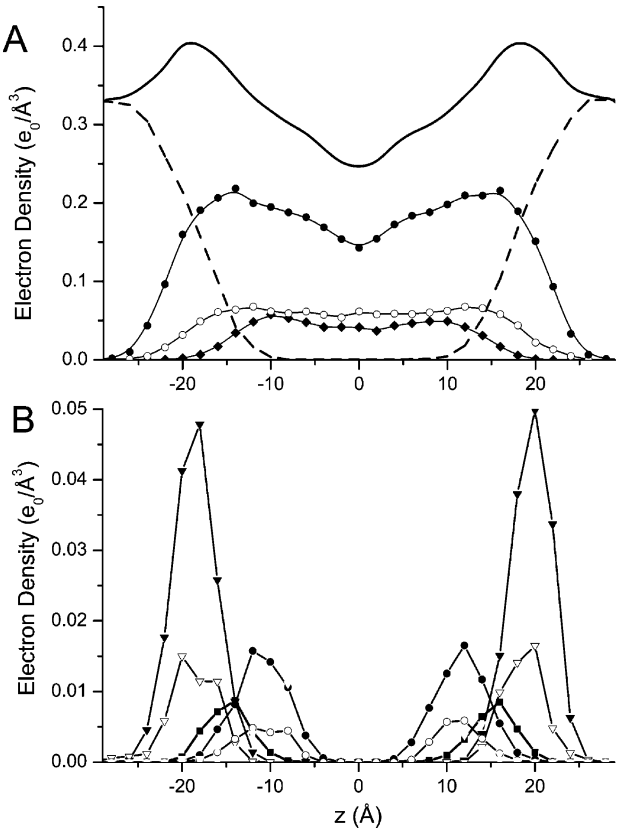

Figure 7. Electron density profiles averaged over the last 1 ns simulation along the bilayer normal. (A) Total simulated system (solid line), water (dashed line), POPC (●), POPA (○), and CHOL (♦); and (B) individual groups of lipids: POPC, phosphorus (▼), POPA phosphorus (▽), hydroxyl oxygen of CHOL (■), C4 of POPC (●), and C4 of POPA (○).

align with C4 atoms and might be responsible for the increase of order at C4.

Conclusions

As revealed by the 50 ns MD simulation, the ternary system of POPC/POPA/CHOL (3:1:1) is heterogeneous in nature. The heterogeneity might result from the inequality of various partnering for interactions. The interaction between the POPA−CHOL seemed to be more favorable than that of the POPC−CHOL. CHOL molecules could form their own dimer complexes, and POPC molecules had their self-enriched domains, but POPA molecules were found to be nowhere closely associated with each other. The heterogeneity might also be contributed by a variety of interactions between molecules, such as VDW, electrostatic, direct hydrogen binding, or water mediated hydrogen binding. The heterogeneous interactions among three different constituents resulted in a broad spectrum of lipid properties, including extensive distributions of average area per lipid and varied lipid ordering as a function of closeness to CHOL.

The ternary system is also characterized by its dynamic structures. Although there was 20% CHOL in the system and these CHOL molecules demonstrated their conventional role of ordering adjacent lipid molecules, the overall population lipids showed great flexibility. This agreed well with the observation that certain population POPA and POPC had relatively large areas per lipid even after 50 ns simulations. The mixture of more and less ordered lipids could form the foundation for the function of nAChR.

Although we cannot assess synergetic effects of POPA and CHOL on nAChR using the present system, the unique lipid mixture prepared in the present study will undoubtedly be valuable for further studies in the presence of nAChR. MD simulations to investigate how POPC/POPA/CHOL (3:1:1) affect the function of nAChR are currently underway in our laboratory.

Acknowledgment. The authors would like to thank Dr. Sagar A. Pandit of Purdue University and Professor John Nagle of Carnegie Mellon University for the stimulating discussions. This material is based upon work supported by the National Science Foundation under the following NSF programs: Partnerships for Advanced Computational Infrastructure, Distributed Terascale Facility (DTF), and Terascale Extensions: Enhancements to the Extensible Terascale Facility. A special acknowledgment goes to the Pittsburgh Supercomputing Center. This research was supported in part by grants from NIH (R01GM066358, R01GM056257, and R37GM049202).

Supporting Information Available: Order parameters of sn1 chain of POPA molecules that were close to CHOL, fraction of gauche bonds, mass densities of water and total lipids along the bilayer normal. This material is available free of charge via the Internet at http://pubs.acs.org.

References and Notes

(1) Lee, A. G. *Biochim. Biophys. Acta* **2003**, *1612*, 1.
(2) Barrantes, F. J. *Brain Res. Rev.* **2004**, *47*, 71.
(3) Miyazawa, A.; Fujiyoshi, Y.; Unwin, N. *Nature* **2003**, *423*, 949.
(4) Unwin, N. *J. Mol. Biol.* **2005**, *346*, 967.
(5) Baenziger, J. E.; Morris, M. L.; Darsaut, T. E.; Ryan, S. E. *J. Biol. Chem.* **2000**, *275*, 777.
(6) Fong, T. M.; McNamee, M. G. *Biochemistry* **1986**, *25*, 830.
(7) Criado, M.; Eibl, H.; Barrantes, F. J. *J. Biol. Chem.* **1984**, *259*, 9188.
(8) Criado, M.; Eibl, H.; Barrantes, F. J. *Biochemistry* **1982**, *21*, 3622.
(9) daCosta, C. J.; Ogrel, A. A.; McCardy, E. A.; Blanton, M. P.; Baenziger, J. E. *J. Biol. Chem.* **2002**, *277*, 201.
(10) Hamouda, A. K.; Sanghvi, M.; Sauls, D.; Machu, T. K.; Blanton, M. P. *Biochemistry* **2006**, *45*, 4327.
(11) daCosta, C. J.; Wagg, I. D.; McKay, M. E.; Baenziger, J. E. *J. Biol. Chem.* **2004**, *279*, 14967.
(12) Fong, T. M.; McNamee, M. G. *Biochemistry* **1987**, *26*, 3871.
(13) Butler, D. H.; McNamee, M. G. *Biochim. Biophys. Acta* **1993**, *1150*, 17.
(14) Jones, O. T.; McNamee, M. G. *Biochemistry* **1988**, *27*, 2364.
(15) Ryan, S. E.; Demers, C. N.; Chew, J. P.; Baenziger, J. E. *J. Biol. Chem.* **1996**, *271*, 24590.
(16) Baenziger, J. E.; Darsaut, T. E.; Morris, M. L. *Biochemistry* **1999**, *38*, 4905.
(17) Scott, H. L. *Curr. Opin. Struct. Biol.* **2002**, *12*, 495.
(18) Marrink, S. J.; Tieleman, D. P. *Biophys. J.* **2002**, *83*, 2386.
(19) Forrest, L. R.; Sansom, M. S. *Curr. Opin. Struct. Biol.* **2000**, *10*, 174.
(20) Humphrey, W.; Dalke, A.; Schulten, K. *J. Mol. Graphics* **1996**, *14*, 33.
(21) Kallen, J. A.; Schlaeppi, J. M.; Bitsch, F.; Geisse, S.; Geiser, M.; Delhon, I.; Fournier, B. *Structure* **2002**, *10*, 1697.
(22) Feller, S. E.; MacKerell, A. D., Jr. *J. Phys. Chem. B* **2000**, *104*, 7510.
(23) Pitman, M. C.; Suits, F.; Mackerell, A. D., Jr.; Feller, S. E. *Biochemistry* **2004**, *43*, 15318.
(24) Kale, L.; Skeel, R.; Bhandarkar, M.; Brunner, R.; Gursoy, A.; Krawetz, N.; Phillips, J.; Shinozaki, A.; Varadarajan, K.; Schulten, K. *J. Comput. Phys.* **1999**, *151*, 283.
(25) Nose, S. *J. Chem. Phys.* **1984**, *81*, 511.
(26) Hoover, W. G. *Phys. Rev. A* **1985**, *31*, 1695.
(27) Brünger, A. *X-PLOR*, Version 3.1: A system for X-ray crystallography and NMR; Yale University: New Haven, 1992.
(28) Darden, T.; York, D.; Pedersen, L. *J. Chem. Phys.* **1993**, *98*, 10089.
(29) Huang, P.; Perez, J. J.; Loew, G. H. *J. Biomol. Struct. Dyn.* **1994**, *11*, 927.
(30) Liu, Z.; Xu, Y.; Tang, P. *Biophys. J.* **2005**, *88*, 3784.
(31) Ruocco, G.; Sampoli, M.; Vallauri, R. *J. Chem. Phys.* **1992**, *96*, 6167.
(32) Jedlovszky, P.; Medvedev, N. N.; Mezei, M. *J. Phys. Chem. B* **2004**, *108*, 465.
(33) Pandit, S. A.; Vasudevan, S.; Chiu, S. W.; Mashl, R. J.; Jakobsson, E.; Scott, H. L. *Biophys. J.* **2004**, *87*, 1092.
(34) Patra, M.; Karttunen, M.; Hyvonen, M. T.; Falck, E.; Lindqvist, P.; Vattulainen, I. *Biophys. J.* **2003**, *84*, 3636.
(35) Shinoda, W.; Okazaki, S. *J. Chem. Phys.* **1998**, *109*, 1517.
(36) Pandit, S. A.; Jakobsson, E.; Scott, H. L. *Biophys. J.* **2004**, *87*, 3312.
(37) Pandit, S. A.; Khelashvili, G.; Jakobsson, E.; Grama, A.; Scott, H. L. *Biophys. J.* **2007**, *92*, 440.
(38) Pasenkiewicz-Gierula, M.; Rog, T.; Kitamura, K.; Kusumi, A. *Biophys. J.* **2000**, *78*, 1376.
(39) Pandit, S. A.; Bostick, D.; Berkowitz, M. L. *Biophys. J.* **2003**, *85*, 3120.
(40) Kucerka, N.; Tristram-Nagle, S.; Nagle, J. F. *J. Membr. Biol.* **2005**, *208*, 193.
(41) Pandit, S. A.; Chiu, S. W.; Jakobsson, E.; Grama, A.; Scott, H. L. *Biophys. J.* **2007**, *92*, 920.
(42) Edholm, O.; Nagle, J. F. *Biophys. J.* **2005**, *89*, 1827.
(43) Ege, C.; Ratajczak, M. K.; Majewski, J.; Kjaer, K.; Lee, K. Y. *Biophys. J.* **2006**, *91*, L01.
(44) Gullingsrud, J.; Schulten, K. *Biophys. J.* **2004**, *86*, 3496.
(45) Rog, T.; Murzyn, K.; Gurbiel, R.; Takaoka, Y.; Kusumi, A.; Pasenkiewicz-Gierula, M. *J. Lipid Res.* **2004**, *45*, 326.
(46) Applegate, K. R.; Glomset, J. A. *J. Lipid Res.* **1991**, *32*, 1635.
(47) Smondyrev, A. M.; Berkowitz, M. L. *J. Chem. Phys.* **1999**, *110*, 3981.
(48) Douliez, J. P.; Ferrarini, A.; Dufourc, E. J. *J. Chem. Phys.* **1998**, *109*, 2513.
(49) Hofsass, C.; Lindahl, E.; Edholm, O. *Biophys. J.* **2003**, *84*, 2192.
(50) Sunshine, C.; McNamee, M. G. *Biochim. Biophys. Acta* **1994**, *1191*, 59.
(51) Patra, M.; Salonen, E.; Terama, E.; Vattulainen, I.; Faller, R.; Lee, B. W.; Holopainen, J.; Karttunen, M. *Biophys. J.* **2006**, *90*, 1121.
(52) Bretscher, M. S.; Munro, S. *Science* **1993**, *261*, 1280.